Real-Time Sediment Plume Modeling in the Southern California Bight

Chinmay S. Kulkarni*, Patrick J. Haley Jr.*, Pierre F. J. Lermusiaux*†, Arkopal Dutt*, Abhinav Gupta*, Chris Mirabito*, Deepak N. Subramani*, Sudip Jana*, Wael H. Ali*, Thomas Peacock*, Carlos Munoz Royo*, Andrew Rzeznik*, Rohit Supekar*

*Department of Mechanical Engineering, Massachusetts Institute of Technology,
77 Massachusetts Avenue, Cambridge, MA 02139
†Corresponding author: pierrel@mit.edu

***Abstract*—With advances in engineering and technology, mining the deep sea for untapped rare metal resources from the bottom of the ocean has recently become economically viable. However, extracting these metal ores from the seabed creates plumes of fine particles that are deposited at various depths within the ocean, and these may be extremely harmful to the marine ecosystems and its components. Thus, for sustainable management, it is of utmost importance to carefully monitor and predict the impact of such harmful activities including plume dispersion on the marine environment. To forecast the plume dispersion in real-time, data-driven ocean modeling has to be coupled with accurate, efficient, and rigorous sediment plume transport computations. The goal of the present paper is to demonstrate the real-time applications of our coupled 3D-and-time data-driven ocean modeling and plume transport forecasting system. Here, the region of focus is the southern California bight, where the PLUMEX 2018 deep sea mining real-time sea experiment was recently conducted (23 Feb - 5 Mar, 2018). Specifically, we demonstrate the improved capabilities of the multiscale MSEAS primitive equation ocean modeling system to capture the complex oceanic phenomenon in the region of interest, the application of the novel method of composition to efficiently and accurately compute the transport of sediment plumes in 3D+1 domains, and the portability of our software and prediction system to different operational regions and its potential in estimating the environmental impacts of deep sea mining activities, ultimately aiding sustainable management and science-based regulations.**

I. Introduction and Motivation

Human activities can irreversibly impact the environment on a global scale. Analyzing and mitigating the impact of such potentially harmful activities is thus a key research thrust. With regard to the oceans, a pressing environmental question is the possible rapid increase in the deep sea mining activities and their impacts on marine life and ecosystems.

Ocean mining sites are vast areas of untapped rare metal resources that have only recently become economically viable. Extracting these metal ores from the seabed creates a plume of fine particles in addition to the discharge plume created during the dewatering process of the ore slurry aboard the ore transport ships [38]. These sediment plumes are deposited at various depths within the ocean and may be extremely harmful to the marine ecosystems and its components [52]. Thus, it is of utmost importance to gauge and mitigate the impact of such harmful activities on the surroundings, either to prevent mining all together and protect ocean regions, or to better manage clean and sustainable mining.

A rigorous approach to monitor and predict the impacts of such activities is to utilize data-driven ocean models for forecasting ocean currents as well as the dispersal of pollutants and contaminants [8, 23, 25]. Further, these pollutant plumes are released at intermediate depths and not necessarily at the ocean floor [38]; the ocean upwelling and currents could carry pollutants upward, out of the deep sea into regions critical to marine food chains. Thus, it is necessary to study the transport of these dynamic plumes in fully three-dimensional domains. Finally, these computations must to be efficient, as the forecast must be issued well in advance to have enough time to take appropriate action.

To this end, we present a novel data-driven ocean forecasting and plume prediction system that is able to accurately forecast the ocean physics (currents, temperature, salinity, dynamic surface height etc.) and sediment plume transport. Our system consists of two parts: *(i)* Our MIT-MSEAS multi-resolution primitive equation regional ocean modeling system [16, 14], which we apply to study and forecast tidal-to-mesoscale processes in the region, including one- and two-way implicit nesting, parameter tuning, data assimilation and data-model comparisons, and *(ii)* a novel plume transport prediction engine that uses the method of composition [18] to compute the transport maps for the potential plume release locations in the considered domain, while using the fields from the regional ocean modeling system as an input. The complete computation is fully three dimensional and is performed in real-time.

Our theory and software were used to guide plume dispersion studies in the PLUMEX 2018 sea exercise (February - March 2018) [13] in the Southern California bight. The goal of this work is to demonstrate the real-time applications of our coupled 3D data-driven ocean modeling and plume transport forecasting system [13] applied to this region of interest. We specifically demonstrate: *(i)* improved capabilities of the MSEAS primitive equation ocean modeling system [16] to capture the complex oceanic phenomenon in the region of interest, *(ii)* application of the recently developed method of composition [18] to efficiently and accurately compute

the transport of sediment plumes in 3D+1 domains, and *(iii)* portability of our software and prediction system to different regions and its potential value in estimating the environmental impacts of deep sea mining activities, aiding in sustainable policy decisions.

The layout of this manuscript is as follows: Section II discusses the primitive equation based regional ocean modeling system, followed by the composition based plume modeling methodology. Section III looks at the results obtained in real-time from our software that were used to guide the PLUMEX sea exercise. We also look at the transport characteristics of the potential plume release sites for a particular release. In Section IV, we compare the results obtained from our model with the experimental data, for an sediment plume released on March 4, 2018 off the coast of San Diego. We draw qualitative conclusions about the accuracy and predictive capabilities of our system from the same. Finally, Section V concludes and summarizes the contributions of this work.

II. Modeling Systems

In this section, we discuss the coupled ocean-plume modeling methodology. First, we describe our implicit 2-way nested, multiscale ocean modeling system with a nonlinear dynamic free surface. Then we outline our composition based plume advection theory and schemes.

A. Multiscale Regional Ocean Modeling System

For the regional ocean modeling and forecasting, we utilize our MSEAS modeling system [16, 28]. MSEAS is used for fundamental research and for realistic simulations and predictions in varied regions of the world's oceans, e.g., [29, 39, 15, 12]. It has also been utilized for fundamental PDE-based path planning of autonomous marine vehicles (e.g., [27, 48, 50, 34]), naval exercises with real-time acoustic ocean predictions [53, 24, 27, 6], and environmental management [7].

At the core of MSEAS is an extensive modeling system for hydrostatic primitive-equation dynamics with a dynamic nonlinear free surface, based on second-order structured finite volumes [16, 14]. It is used to study and quantify tidal-to-mesoscale processes over regional domains with complex geometries and varied interactions. The MSEAS capabilities include: fast-marching coastal objective analysis [3]; estimation of spatial and temporal scales from data [2]; initializations of fields and ensembles [20, 14]; nested data-assimilative tidal prediction and inversion [33]; implicit two-way nesting and tiling [16]; stochastic subgrid-scale models [21]; path planning [37, 34, 49, 48, 19, 24]; Lagrangian Coherent Structures; non-Gaussian data assimilation and adaptive sampling [46, 47, 36, 35, 22]; dynamically-orthogonal equations for uncertainty predictions [41, 42, 51]; Lagrangian coherent structures and their uncertainties [26]; and machine learning of model formulations.

B. Plume Modeling System

Once the forecast of the ocean fields is produced by the MSEAS modeling system, it is fed as an input to the plume advection computation engine. Given the initial location of the plume and the location and the intensity of the source, if any, the temporal evolution of the plume is computed using a novel composition-based advection methodology [18].

As the entire system is developed to support real-time marine experiments, our focus is not only on rigorous theory but also on efficient and flexible computation. As mentioned earlier, due to the various constraints during real-time sea experiments, forecasts need to be available for a variety of start times, monitoring durations, and at multiple potential release locations. Our novel methodology is able to account for all these requirements with minimal extra computations.

We assume that the plumes released from the deep sea mining operations are passively advected by the background ocean currents (*e.g.* [5]). We denote the plume concentration by $\alpha(x,t)$, with the initial concentration being $\alpha_0(x)$. The transport of the sediment plume is governed by the advective-transport equation (1).

$$\frac{\partial \alpha(x,t)}{\partial t} + v(x,t) \cdot \nabla \alpha(x,t) = S_\alpha(x,t)\,, \tag{1}$$

where $v(x,t)$ is the unsteady velocity field, obtained from the multi-resolution primitive equation ocean model and $S_\alpha(x,t)$ denotes the source(s) of the plume concentration. It is assumed that the potential sites of plume generation and the generation rates are known a priori. In order to solve this equation efficiently, we make use of the method of compositions [18], which is based on Lagrangian flow maps suitably adapted to accommodate tracer advection. The flow map is a mapping of the initial material element positions to their later positions at the end time under the advective action of the velocity field. The (backward) flow map of a dynamical system governed by the velocity field $v(x,t)$ is given by equation

$$\phi_t^0(x) = x_0\,, \text{ where } \frac{dx}{dt} = v(x(t),t) \text{ with } x(0) = x_0\,. \tag{2}$$

The connection between equations (1) and (2) can be studied by looking at the motion of an individual fluid parcel that is initially at x_0. This parcel is carrying with it the tracer value $\alpha_0(x_0)$ and moves due to the velocity field $v(x(t),t)$, while tracer is added at the rate of $S_\alpha(x(t),t)$ to this parcel. The partial differential equation (PDE) (1) implicitly solves the ODE (2) for all admissible initial positions x_0. That is, the ODE (2) is a characteristic of the PDE (3) [31].

In order to compute the flow map, we make use of equation (1), with the initial condition $\alpha_0(x) = x$ [30, 11, 18]. This computation of the flow map can be modified suitably to account for the different boundary conditions of inflows and outflows, as described in [18].

Computing the flow maps over different subintervals of a larger parent time interval, i.e., the interval within which all the intervals of interest lie, requires multiple independent computations. This is a major disadvantage in the case of providing predictive support for real-time sea operations, as it is imperative to be flexible in terms of the start times as well as the time intervals of interest. This difficulty is overcome by using the idea of composing flow maps [4]. Let us denote the

discretized time interval by the index i; spanning from 0 to $n = t/\Delta t$, where Δt is the timestep. Then the flow map ϕ_n^0 can be expressed as

$$\phi_n^0(x) = \phi_1^0\left(\phi_2^1\left(\dots\phi_n^{n-1}\left(x\right)\right)\right) . \tag{3}$$

Here, note that $\phi_i^{i-1}(x) = \phi_{i\Delta t}^{(i-1)\Delta t}$. Numerically, the composition of individual flow maps is computed using suitable interpolation schemes. It has also been proven that the accuracy of the flow map computation and the tracer advection is maintained given that the order of interpolation is the same or higher than that of the numerical advection schemes [18, 54]. The final advected plume field is given by equation (4).

$$\alpha(x,t) = \alpha_0\left(\phi_1^0\left(\phi_2^1\left(\dots\phi_n^{n-1}\left(x\right)\right)\right)\right) \tag{4}$$

A pictorial description of the composition based computational methodology is presented in Fig. 1.

Computing plume transport through this methodology presents several advantages especially to support real-time sea experiments. First, all the individual flow map computations are completely independent of each other, and hence that allows the computations be carried out in parallel in a distributed computing setup. The other advantage of the fact that these computations are independent is that the numerical errors in the flow map computations are not compounded in time and thus the results are more accurate. Finally, the computation is flexible in terms of the start time and also the time duration, as it only requires composition of the corresponding flow maps, which are already computed (as opposed to re-solving the equations (1)). For example, we assume the parent time interval to be $[0, n\Delta t]$. Then, we pre-compute all the flow maps $\phi_1^0, \phi_2^1, \dots, \phi_{n-2}^{n-1}, \phi_{n-1}^n$. If tracer advection from time $t_s = n_s\Delta t$ to $t_e = n_e\Delta t$ is desired, we simply compute it as given by

$$\alpha(x,t_e) = \alpha_{t_s}\left(\phi_{n_s+1}^{n_s}\left(\phi_{n_s+2}^{n_s+1}\left(\dots\phi_{n_e}^{n_e-1}\left(x\right)\right)\right)\right) . \tag{5}$$

Most importantly, this computation requires only additional interpolations, and no new PDE solves that can be computationally expensive. Currently we only model the dispersion of the plume as an advective transport process. However, other models such as the advection-diffusion model [55], advection-diffusion with settling [17] can be readily incorporated in the composition based model and is a possible direction for future work.

The computation to (1) for computing the individual flow maps is carried out on a collocated Cartesian grid, with 5^{th} order weighted essentially non-oscillatory (WENO) scheme [43, 44] for the spatial gradients and 3^{rd} order total variation diminishing Runge-Kutta (TVD-RK3) scheme [40] for time marching. Interpolation schemes of appropriate order are used to compose these individual flow maps. The velocity output of the ocean model is interpolated four times in each direction for higher resolution. The setup is run on a computing cluster with 24 cores and 256GB RAM and it takes about 25 minutes of computation per model day.

III. Real-Time Results in the Southern California Bight

Our modeling systems and software were employed to forecast the sediment plume transport in the southern California bight during the PLUMEX sea exercise. This sea exercise occurred from February 23 to March 05 2018 in the Pacific ocean off the coast of San Diego. As a part of this experiment, sediment plumes mimicking the those generated from deep sea mining activities were released and tracked. The results provide insights into the behavior of such plumes and form the basis of our understanding of the potential environmental impacts of deep sea mining activities. The experiments were performed aboard the research vessel Sally Ride [1], and dewatering plumes of density $1030.4\ kg/m^3$ were utilized. The plumes were tracked using transmissometers. CTD and ADCP profiling was used to measure the velocities around the vessel, and were utilized in real-time to correct the ocean forecasts. The plume releases were planned at the marked locations at depths of $60\ m$, $80\ m$ and $140\ m$ below the ocean surface and the plumes were observed up to 8 hours.

The modeling domain is off the coast of San Diego, with an area $687\ km \times 720\ km$ as shown in Figure. 2. The red dashed lines in Fig. 2 show the special focus area around the gulf of San Catalina, where most of the at-sea experimental work occurred. For the real-time ocean forecasting, the MSEAS modeling system was set up with 2-way nesting with resolutions of $1.5\ km$ and $0.5\ km$ for the full and nested domains (the special focus area within the dashed red line in Fig. 2) respectively and 100 optimized terrain following vertical levels. The computational domain is a rotated spherical grid, rotated by an angle 35° for optimal computations. The model bathymetry used is obtained from the 15 arcseconds SRMT15 data set [45]. The tidal forcing fields were computed from the high resolution TPXO8-Atlas from OSU [10, 9] and reprocessed for the higher resolution bathymetry [32] and nonlinear bottom drag. The forecasts were initialized from the $1/12^\circ$ HYCOM (Hybrid Coordinate Ocean Model) analysis fields, but with updates based on varied in-situ and remote data of opportunity and assimilating the PLUMEX data and other observations in real-time.

The velocity fields as well as the plume transport forecasts were issued a day in advance and an updated forecast for the day was issued early in the morning, through the MSEAS sea exercise web interface [13]. Fig. 3 shows sample snapshots of this web interface. We predict the ocean physics fields including velocity, vorticity, temperature and salinity in three dimensions in the full Southern California modeling domain, around the gulf of San Catalina region, off San Diego and around the San Clemente island. The sediment transport is also predicted in real-time and reported in two ways: horizontal transport maps at different depths and fully three-dimensional plots. We predicted the plume transport for different start times ranging from 8:00AM PST to 8:00PM PST, starting every hour. The intervals for plume tracking were up to 12 hours.

Let us now focus on a single plume release case to quali-

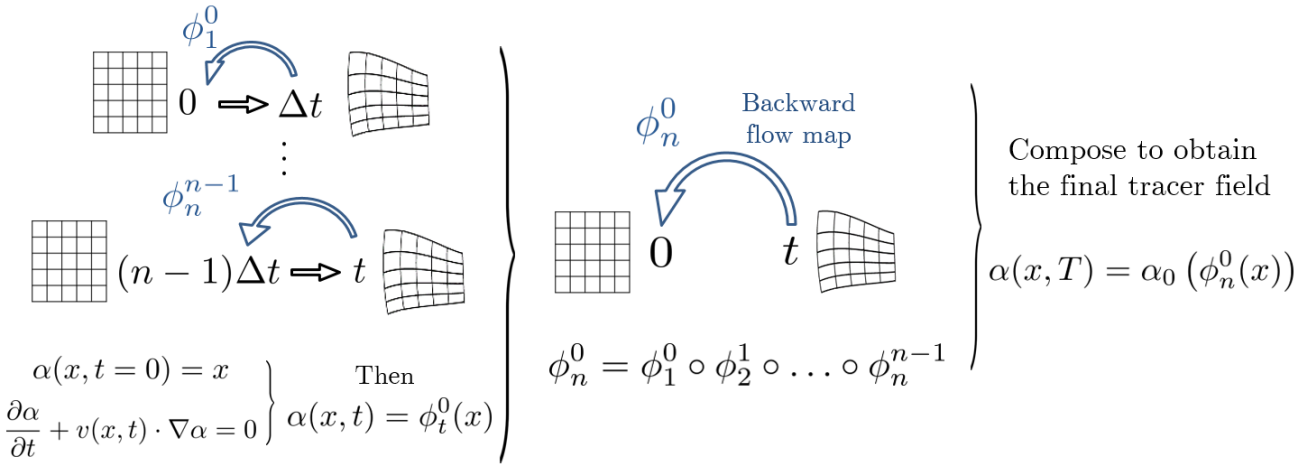

Fig. 1: Composition based plume advection methodology. The first step involves computing the individual flow maps (while accounting for boundary conditions), which can be done in parallel. The second step then involves computing the cumulative flow map over the entire time interval, and the final step involves composing this computed flow map with the initial plume (tracer) field to obtain the final plume field.

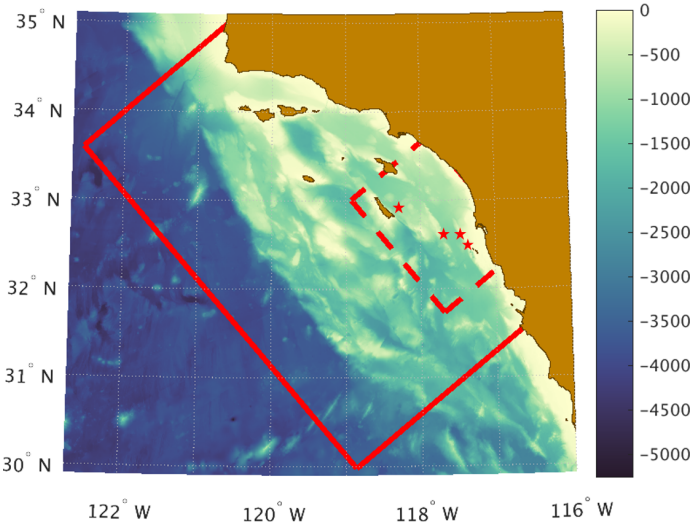

Fig. 2: The MIT-MSEAS modeling domain for the PLUMEX 2018 sea exercises, along with the bathymetry of the region. The solid red line denotes the computational domain and the dashed red line demarcates the special focus area around the gulf of San Catalina. The red stars indicate potential plume release locations.

tatively better understand the dynamics of the two and three-dimensional dispersion as well as the characteristics of the transport from the three potential locations. We consider the plume release on March 4, 2018 at 2:00PM PST, where the plume is tracked for 12 hours. Fig. 4 shows the plume transport in a two-dimensional setting at a depth of $140\ m$. Fig. 5 shows the fully three-dimensional evolution of the plume, assuming the plume was again released at $140\ m$ below the ocean surface.

It can be clearly seen that all the plumes are generally forecast to be transported to the south due to the ocean currents. Plumes from the two central locations are advected more as the strength of currents in this region is higher as compared to the currents near the California coast or around the San Clemente island. As can be seen from Figs. 4 and 5, the latter forecast captures the vertical transport of the plumes, which is quite substantial for the two eastern release locations; however the releases in the deeper ocean travel in the vertical direction in a more coherent fashion. For example, the release closest to the California coast is dispersed for about $50\ m$ in the vertical. This is mainly because of the upwelling zones near the coast and bathymetric effects. The typical instrumentation utilized to experimentally observe such plumes performs a yo-yo motion in the vertical; hence quantifying and predicting the vertical transport of the plume is imperative. This is the primary reason why it is necessary to predict the dispersion in three dimensions as opposed to predictions at fixed depth. Another approach can be to perform two-dimensional plume transport prediction along isopycnals, assuming that the sediment settles and is transported along these surfaces of constant density.

IV. Comparison with Experimental Data

We now look at the skill of predictions for the experiment that was conducted on 2:11PM PST on March 4

Real-time MSEAS Forecasting

▪ MSEAS Ocean Forecasts

Real-Time Forecast Estimates of Present (06 Mar 1800Z) Environmental Conditions						
Gulf of Santa Catalina (GSC) Domain (0.5 km resolution, Implicit-2-way Nested)				Off San Diego	GSC Southern Section (0.5 km resolution)	
0m Temperature	2m Vorticity	140m Temperature	140m Velocity	140m Temperature	Temperature	Salinity
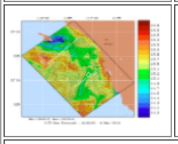	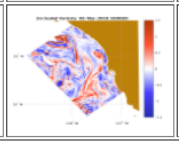	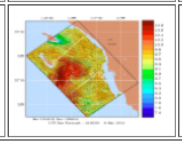	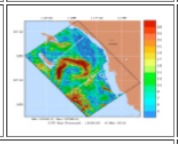	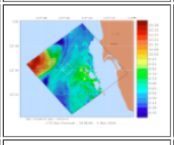	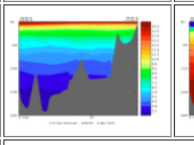	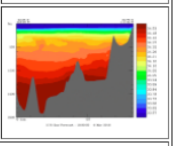
Southern California (SC) Domain (1.5 km resolution, Implicit-2-way Nested)				San Clemente Island	California Current Section (1.5 km resolution)	
0m Temperature	2m Vorticity	140m Temperature	140m Velocity	140m Temperature	Temperature	Salinity
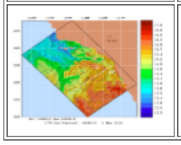	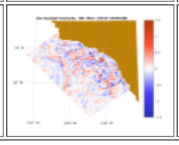	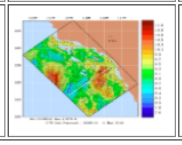	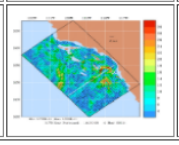	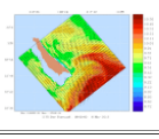	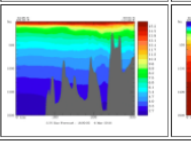	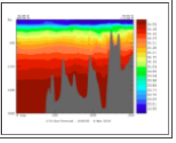

Nowcast and Forecast Products with dynamics descriptions			Analyses and Forecasts Issued On									
			February 2018						March 2018			
			23	24	25	26	27	28	1	2	3	4	5
Ocean Physics	Horizontal Maps	Central Forecast	X	X	X	X	X	X	X	X	X	X	X
		Plumes Area Central Forecast				X	X	X	X	X	X	X	X
	Operational Vertical Section	Central Forecast	X	X	X	X	X	X	X	X	X	X	X
Sediment Transport and Coherent Structures	Horizontal Maps	Central Forecast					X	X		X	X	X	X
	3D Maps	Central Forecast							X		X	X	X

▪ MSEAS-processed atmospheric forcing flux forecasts:

NCEP NAM 3km	February/March 2018										
Daily average wind stress, E-P, heat flux, and SW Radiation											
MSEAS-processed NCEP Flux Forecast snapshot plots	X	X	X	X	X	X	X	X	X	X	X
Forecast snapshot plots	23	24	25	26	27	28	1	2	3	4	5

(a) The MIT-MSEAS parent web interface

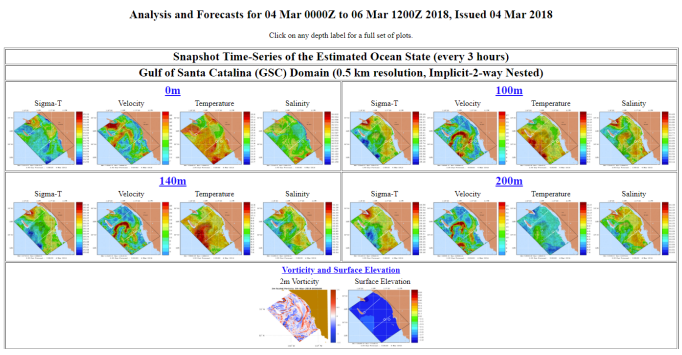

(b) Snapshots of the ocean physics forecast fields page

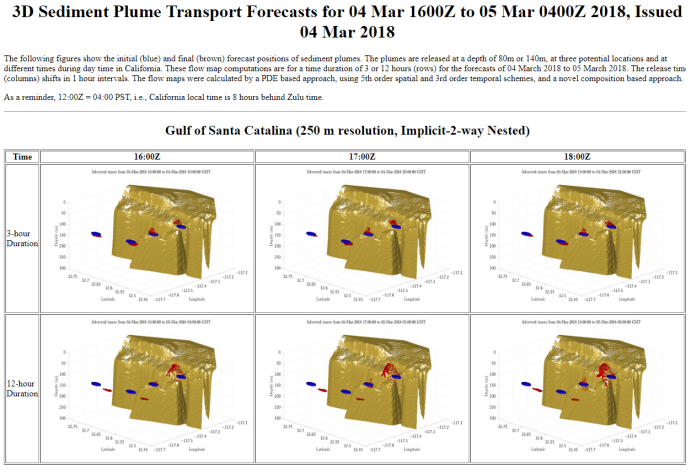

(c) Snapshot of the fully three-dimensional plume transport forecast page

Fig. 3: MIT-MSEAS real-time sea exercise portal for PLUMEX 2018 (http://mseas.mit.edu/Sea_exercises/DeepSeaMining)

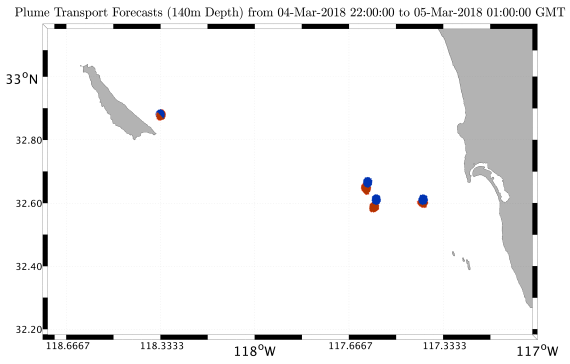

Fig. 4: Plume transport forecast over 3 hours in two dimensions at a depth of 140 m. The initial plume release markers are in blue and the final transported plume is in red.

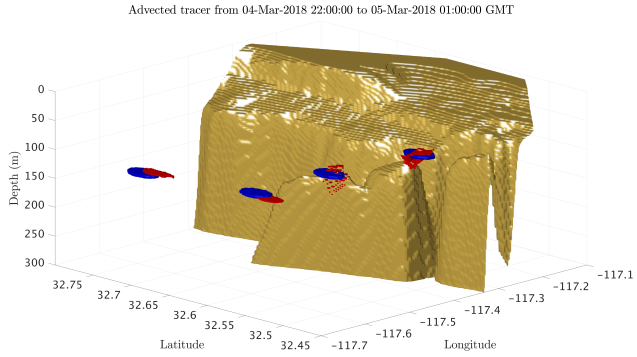

Fig. 5: Plume transport forecast over 3 hours in three dimensions. The plume was released at a depth of 140 m. The initial plume release markers are in blue and the final transported plume is in red.

2018. Here, a sediment plume of density 1030.4 kg/m^3 was released at a depth of 59 m. The release location was $32.6920°N,\ 117.6126°W$. The plume was tracked for 380 minutes by using the shipboard transmissometer. The release location along with the ship path are shown in Fig. 6.

In order to retrospectively test our predictive skill as well as modeling accuracy, we did a hindcast study mimicking this plume release. In order to obtain the plume transport at a comparable scale to the ship movement, we interpolate the original velocity field obtained from the primitive equation solver by eight times in each direction.

Figures 7 and 8 consolidate the results from the data collected aboard *R/V Sally Ride* and the hindcast computation. Figure 7 shows the results from the transmissometer data with depth and time (from the plume release time) along the ship path. Low values of transmission indicate the plume location. We notice the that the plume travels towards the southeast, but largely remains at the depth that it was released. Figure 8 shows the predicted location of the hindcast plume 2 hours post the release, as a large part of the plume was

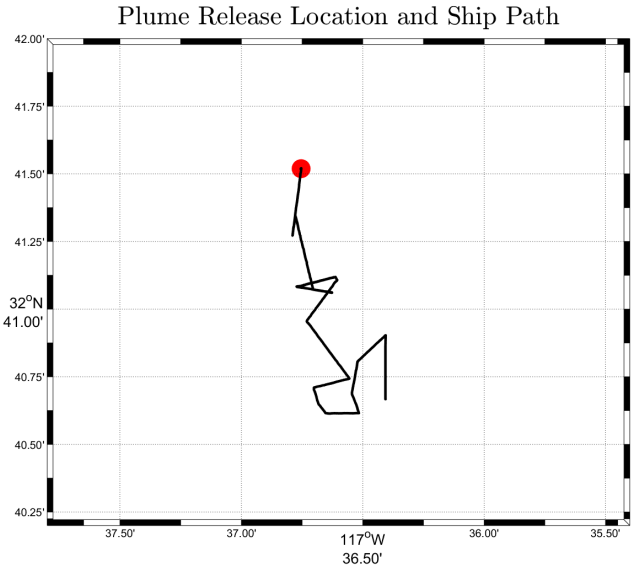

Fig. 6: The plume release location and the ship track. The sediment plume was released at the red marker at 2:11PM PST on March 5 2018. The plume was tracked using the shipboard transmissometer where the ship followed the path shown in black.

tracked around this time, as seen from Figure 7. The dotted circle denotes the general region in which the plume was experimentally observed. Note that this region is only an approximation for such a region, as the plume could only have been observed and sampled along the ship track. The ship path is overlaid in red.

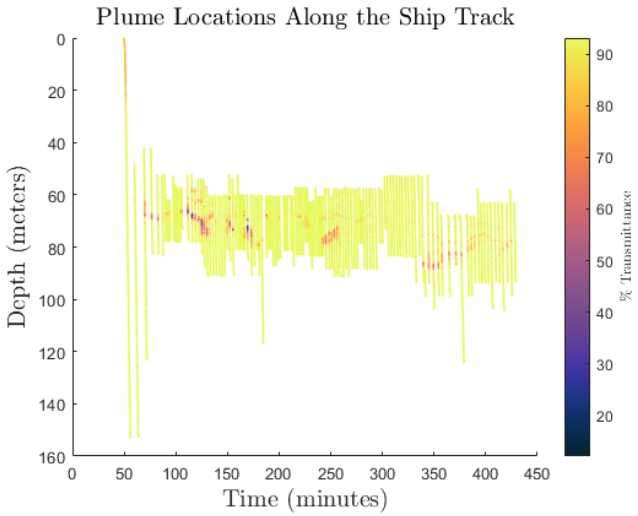

Fig. 7: Observed sediment plume location along the ship track using the transmissometer. Low values of transmittance indicate the sediment plume.

It can be clearly seen that the predicted transport of the plume is towards the south-southeast, which is corroborated by the experiments. Further, the part of the ship track where

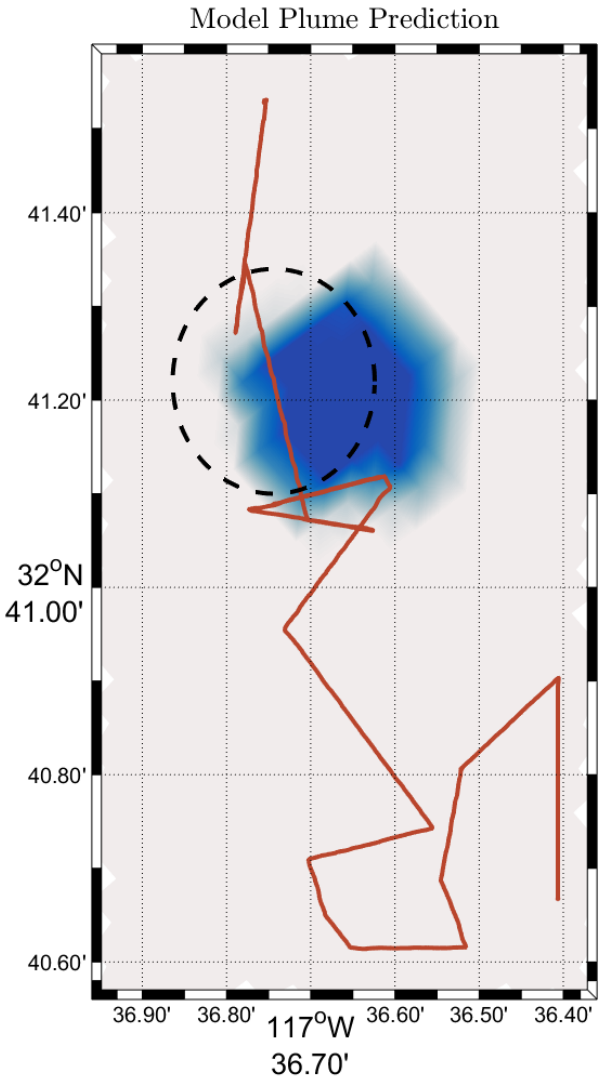

Fig. 8: Predicted plume location (in blue). The dotted circle denotes the approximate area in which the plume was observed. The ship track is overlaid in red.

majority of the plume was observed indeed passes through the region of the forecasted plume location. This serves as an ideal validation of the modeling methodology, the computational setup as well as the software application of our system.

V. Conclusions

This work presents an effective integrated methodology to predict the transport of sediment plumes arising from deep sea mining operations along with its real-time operation conducted as a part of the PLUMEX 2018 [13] sea exercise. The integrated system is able to forecast the ocean fields as well as sediment plume transports in real-time which can be used predict, monitor and mitigate the environmental impact of deep sea mining activities. The presented real-time exercise proved the viability of our coupled data-driven ocean field forecasting and plume transport methodology in real-time.

We first discussed the results of our multi-resolution regional ocean modeling system in the southern California Bight that is sufficiently resolved for use in monitoring and forecasting the regional transport of material arising from deep sea mining operations. Using the implicit 2-way nesting of the MSEAS modeling system, we downscaled initial conditions from an operational global model (HYCOM) and tidal forcing from the global TPXO8 Atlas, but processed for high-resolution bathymetry and nonlinear dynamics. We also updated the downscaled fields based on a range of observations of opportunity, varied MIT-MSEAS feature models, and data collected by the PLUMEX sea exercise. The results showed that the MIT-MSEAS system was able to successfully forecast the regional ocean fields for use in Lagrangian transports. Quantitative guidance on ocean dynamics, optimal sediment plume deployments, and optimal adaptive sampling was also provided and used in real-time.

The second part of the methodology uses the forecast multiscale ocean fields to predict and characterize the transport of the sediment plume. We discussed the fundamentals of the novel composition based advection methodology that enables efficient, accurate and flexible computation in fully three-dimensional domains, as the plumes may be displaced vertically due to upwelling / downwelling as well as buoyancy effects. The resulting ocean physics as well as the plume transport maps were used to guide the planning and execution of the plume transport studies during the PLUMEX 2018 sea exercise. Specifically, we examined the transport characteristics of the four proposed plume release locations for varied initial release times spanning a week. Finally, to determine the quality of our system, we looked at the experimental data obtained from the plume release on March 4 2018 and compared it with the hindcast results obtained from our model for the exact same set of parameters. It was observed that the plume travels southeast from the release point over a duration of about 6 hours. Although our model uses a coarse resolution for the experimental length scales, we observed a good qualitative prediction with respectable accuracy, which showcased the precision and the usability of our model. Finally, the accuracy, efficiency, and the portability of our integrated software makes it a very valuable asset for the real-time monitoring, forecasting, and control of the possibly adverse environmental impacts of deep sea mining activities.

Acknowledgment

We thank the members of the MSEAS group for useful discussions. We are grateful to the MIT Environmental Solutions Initiative (MIT-ESI) for Seed Grant research support. We also thank the Office of Naval Research (ONR) and the National Oceanographic Partnership Program (NOPP) for enabling our MSEAS modeling system development and for research support under grant N00014-15-1-2597 (Seamless Multiscale Forecasting) to the Massachusetts Institute of Technology (MIT). We thank Matthew Alford from Scripps for his close collaboration in this project, and his group and Scripps personnel for providing CTD, ADCP, and plume data

from R/V Sally Ride. We thank our partners from Global Sea Mineral Resources (GSR) and the International Seabed Authority (ISA) for their collaboration. We wish to thank Matthew Pyle, Eric Rogers, Geoff DiMego, and Arun Chawla of NCEP for help and support for atmospheric forcing data, NOAA for supplying buoy data, NASA JPL for supplying SST data, and the Coastal Observing Research and Development Center (CORDC) and Scripps for supplying HF Radar data.

REFERENCES

[1] R/V Sally Ride, UC San Diego; https://scripps.ucsd.edu/ships/sally-ride.

[2] A. Agarwal. Statistical Field Estimation and Scale Estimation for Complex Coastal Regions and Archipelagos. Master's thesis, Massachusetts Institute of Technology, Department of Mechanical Engineering, Cambridge, Massachusetts, May 2009.

[3] A. Agarwal and P. F. J. Lermusiaux. Statistical field estimation for complex coastal regions and archipelagos. *Ocean Modelling*, 40(2):164–189, 2011.

[4] Steven L Brunton and Clarence W Rowley. Fast computation of finite-time lyapunov exponent fields for unsteady flows. *Chaos: An Interdisciplinary Journal of Nonlinear Science*, 20(1):017503, 2010.

[5] Richard Camilli, Christopher M Reddy, Dana R Yoerger, Benjamin AS Van Mooy, Michael V Jakuba, James C Kinsey, Cameron P McIntyre, Sean P Sylva, and James V Maloney. Tracking hydrocarbon plume transport and biodegradation at deepwater horizon. *Science*, 330(6001):201–204, 2010.

[6] L. R. Centurioni et al. Northern Arabian Sea circulation-autonomous research (NASCar): A research initiative based on autonomous sensors. *Oceanography*, 30(2):74–87, June 2017. Special issue on Autonomous and Lagrangian Platforms and Sensors (ALPS).

[7] G. Cossarini, P. F. J. Lermusiaux, and C. Solidoro. Lagoon of Venice ecosystem: Seasonal dynamics and environmental guidance with uncertainty analyses and error subspace data assimilation. *Journal of Geophysical Research: Oceans*, 114(C6), June 2009.

[8] J. Coulin, P. J. Haley, Jr., S. Jana, C. S. Kulkarni, P. F. J. Lermusiaux, and T. Peacock. Environmental ocean and plume modeling for deep sea mining in the bismarck sea. In *Oceans 2017 - Anchorage*, Anchorage, AK, September 2017.

[9] Gary D Egbert and Svetlana Y Erofeeva. Efficient inverse modeling of barotropic ocean tides. *Journal of Atmospheric and Oceanic Technology*, 19(2):183–204, 2002.

[10] Gary D Egbert and Svetlana Y Erofeeva. OSU tidal inversion. http://volkov.oce.orst.edu/tides/tpxo8_atlas.html, 2013.

[11] Florian Feppon and Pierre F. J. Lermusiaux. Dynamically orthogonal numerical schemes for efficient stochastic advection and Lagrangian transport. *SIAM Review*, 60(3):595–625, 2018.

[12] Avijit Gangopadhyay, Pierre F.J. Lermusiaux, Leslie Rosenfeld, Allan R. Robinson, Leandro Calado, Hyun Sook Kim, Wayne G. Leslie, and Patrick J. Haley, Jr. The California Current system: A multiscale overview and the development of a feature-oriented regional modeling system (FORMS). *Dynamics of Atmospheres and Oceans*, 52(1–2):131–169, September 2011. Special issue of Dynamics of Atmospheres and Oceans in honor of Prof. A. R. Robinson.

[13] MSEAS Group. Deep sea mining sea experiment 2018; http://mseas.mit.edu/Sea_exercises/DeepSeaMining/.

[14] P. J. Haley, Jr., A. Agarwal, and P. F. J. Lermusiaux. Optimizing velocities and transports for complex coastal regions and archipelagos. *Ocean Modeling*, 89:1–28, 2015.

[15] P. J. Haley, Jr., P. F. J. Lermusiaux, A. R. Robinson, W. G. Leslie, O. Logoutov, G. Cossarini, X. S. Liang, P. Moreno, S. R. Ramp, J. D. Doyle, J. Bellingham, F. Chavez, and S. Johnston. Forecasting and reanalysis in the Monterey Bay/California Current region for the Autonomous Ocean Sampling Network-II experiment. *Deep Sea Research Part II: Topical Studies in Oceanography*, 56(3–5):127–148, February 2009.

[16] Patrick J. Haley, Jr. and Pierre F. J. Lermusiaux. Multiscale two-way embedding schemes for free-surface primitive equations in the "Multidisciplinary Simulation, Estimation and Assimilation System". *Ocean Dynamics*, 60(6):1497–1537, December 2010.

[17] JA Jankowski, A Malcherek, and W Zielke. Numerical modeling of suspended sediment due to deep-sea mining. *Journal of Geophysical Research: Oceans*, 101(C2):3545–3560, 1996.

[18] Chinmay S. Kulkarni and Pierre F. J. Lermusiaux. Accurate and efficient advection schemes through pde-based flow map composition. 2018. In preparation.

[19] Chinmay Sameer Kulkarni. Three-dimensional time-optimal path planning in dynamic and realistic environments. Master's thesis, Massachusetts Institute of Technology, Department of Mechanical Engineering, Cambridge, Massachusetts, June 2017.

[20] P. F. J. Lermusiaux. On the mapping of multivariate geophysical fields: Sensitivities to size, scales, and dynamics. *Journal of Atmospheric and Oceanic Technology*, 19(10):1602–1637, 2002.

[21] P. F. J. Lermusiaux. Uncertainty estimation and prediction for interdisciplinary ocean dynamics. *Journal of Computational Physics*, 217(1):176–199, 2006.

[22] P. F. J Lermusiaux. Adaptive modeling, adaptive data assimilation and adaptive sampling. *Physica D: Nonlinear Phenomena*, 230(1):172–196, 2007.

[23] P. F. J. Lermusiaux, C.-S. Chiu, G. G. Gawarkiewicz, P. Abbot, A. R. Robinson, R. N. Miller, P. J. Haley, Jr, W. G. Leslie, S. J. Majumdar, A. Pang, and F. Lekien. Quantifying uncertainties in ocean predictions. *Oceanography*, 19(1):92–105, 2006.

[24] P. F. J. Lermusiaux, P. J. Haley, Jr., S. Jana, A. Gupta,

C. S. Kulkarni, C. Mirabito, W. H. Ali, D. N. Subramani, A. Dutt, J. Lin, A. Shcherbina, C. Lee, and A. Gangopadhyay. Optimal planning and sampling predictions for autonomous and lagrangian platforms and sensors in the northern Arabian Sea. *Oceanography*, 30(2):172–185, June 2017. Special issue on Autonomous and Lagrangian Platforms and Sensors (ALPS).

[25] P. F. J Lermusiaux, P. J. Haley, Jr, and N. K. Yilmaz. Environmental prediction, path planning and adaptive sampling: sensing and modeling for efficient ocean monitoring, management and pollution control. *Sea Technology*, 48(9):35–38, 2007.

[26] P. F. J. Lermusiaux and F. Lekien. Dynamics and Lagrangian coherent structures in the ocean and their uncertainty. In Jerrold E. Marsden and Jurgen Scheurle, editors, *Extended Abstract in report of the Dynamical System Methods in Fluid Dynamics Oberwolfach Workshop*, page 2, Germany, July 31st - August 6th 2005. Mathematisches Forschungsinstitut Oberwolfach.

[27] P. F. J. Lermusiaux, D. N. Subramani, J. Lin, C. S. Kulkarni, A. Gupta, A. Dutt, T. Lolla, P. J. Haley, Jr., W. H. Ali, C. Mirabito, and S. Jana. A future for intelligent autonomous ocean observing systems. *Journal of Marine Research*, 75(6):765–813, November 2017. The Sea. Volume 17, The Science of Ocean Prediction, Part 2.

[28] W. G. Leslie, P. J. Haley, Jr., P. F. J. Lermusiaux, M. P. Ueckermann, O. Logutov, and J. Xu. MSEAS Manual. MSEAS Report 06, Department of Mechanical Engineering, Massachusetts Institute of Technology, Cambridge, MA, 2010.

[29] W. G. Leslie, A. R. Robinson, P. J. Haley, Jr, O. Logutov, P. A. Moreno, P. F. J. Lermusiaux, and E. Coelho. Verification and training of real-time forecasting of multiscale ocean dynamics for maritime rapid environmental assessment. *Journal of Marine Systems*, 69(1):3–16, 2008.

[30] Shingyu Leung. An eulerian approach for computing the finite time lyapunov exponent. *Journal of computational physics*, 230(9):3500–3524, 2011.

[31] Randall J LeVeque. *Finite volume methods for hyperbolic problems*, volume 31. Cambridge university press, 2002.

[32] O. G. Logutov and P. F. J. Lermusiaux. Inverse barotropic tidal estimation for regional ocean applications. *Ocean Modelling*, 25(1–2):17–34, 2008.

[33] Oleg G. Logutov. A multigrid methodology for assimilation of measurements into regional tidal models. *Ocean Dynamics*, 58(5–6):441–460, December 2008.

[34] T. Lolla, P. J. Haley, Jr., and P. F. J. Lermusiaux. Time-optimal path planning in dynamic flows using level set equations: Realistic applications. *Ocean Dynamics*, 64(10):1399–1417, 2014.

[35] T. Lolla and P. F. J. Lermusiaux. A Gaussian mixture model smoother for continuous nonlinear stochastic dynamical systems: Applications. *Monthly Weather Review*, 145:2763–2790, July 2017.

[36] T. Lolla and P. F. J. Lermusiaux. A Gaussian mixture model smoother for continuous nonlinear stochastic dynamical systems: Theory and scheme. *Monthly Weather Review*, 145:2743–2761, July 2017.

[37] T. Lolla, P. F. J. Lermusiaux, M. P. Ueckermann, and P. J. Haley, Jr. Time-optimal path planning in dynamic flows using level set equations: Theory and schemes. *Ocean Dynamics*, 64(10):1373–1397, 2014.

[38] Kathryn Miller, Kirsten Thompson, Paul Johnston, and David Santillo. An overview of seabed mining including the current state of development, environmental impacts and knowledge gaps. *Frontiers in Marine Science*, 4:418.

[39] Reiner Onken, Allan R. Robinson, Pierre F. J. Lermusiaux, Patrick J. Haley, and Larry A. Anderson. Data-driven simulations of synoptic circulation and transports in the Tunisia-Sardinia-Sicily region. *Journal of Geophysical Research: Oceans*, 108(C9), 2003.

[40] Stanley Osher and Ronald Fedkiw. *Level set methods and dynamic implicit surfaces*, volume 153. Springer Science & Business Media, 2006.

[41] Themistoklis P. Sapsis and Pierre F. J. Lermusiaux. Dynamically orthogonal field equations for continuous stochastic dynamical systems. *Physica D: Nonlinear Phenomena*, 238(23–24):2347–2360, December 2009.

[42] Themistoklis P. Sapsis and Pierre F. J. Lermusiaux. Dynamical criteria for the evolution of the stochastic dimensionality in flows with uncertainty. *Physica D: Nonlinear Phenomena*, 241(1):60–76, 2012.

[43] Chi-Wang Shu. Essentially non-oscillatory and weighted essentially non-oscillatory schemes for hyperbolic conservation laws. In *Advanced numerical approximation of nonlinear hyperbolic equations*, pages 325–432. Springer, 1998.

[44] Chi-Wang Shu. High order eno and weno schemes for computational fluid dynamics. In *High-order methods for computational physics*, pages 439–582. Springer, 1999.

[45] Walter HF Smith and David T Sandwell. Global sea floor topography from satellite altimetry and ship depth soundings. *Science*, 277(5334):1956–1962, 1997.

[46] T. Sondergaard and P. F. J. Lermusiaux. Data assimilation with Gaussian Mixture Models using the Dynamically Orthogonal field equations. Part I: Theory and scheme. *Monthly Weather Review*, 141(6):1737–1760, 2013.

[47] T. Sondergaard and P. F. J. Lermusiaux. Data assimilation with Gaussian Mixture Models using the Dynamically Orthogonal field equations. Part II: Applications. *Monthly Weather Review*, 141(6):1761–1785, 2013.

[48] D. N. Subramani, P. J. Haley, Jr., and P. F. J. Lermusiaux. Energy-optimal path planning in the coastal ocean. *Journal of Geophysical Research: Oceans*, 122:3981–4003, 2017.

[49] D. N. Subramani and P. F. J. Lermusiaux. Energy-optimal path planning by stochastic dynamically orthogonal level-set optimization. *Ocean Modeling*, 100:57–77, 2016.

[50] D. N. Subramani, P. F. J. Lermusiaux, P. J. Haley,

Jr., C. Mirabito, S. Jana, C. S. Kulkarni, A. Girard, D. Wickman, J. Edwards, and J. Smith. Time-optimal path planning: Real-time sea exercises. In *Oceans '17 MTS/IEEE Conference*, Aberdeen, June 2017.

[51] M. P. Ueckermann, P. F. J. Lermusiaux, and T. P. Sapsis. Numerical schemes for dynamically orthogonal equations of stochastic fluid and ocean flows. *Journal of Computational Physics*, 233:272–294, January 2013.

[52] A Vanreusel, A Hiliario, PA Ribeiro, L Menot, and P Arbizu Martinez. Managing impacts of deep sea resource exploitation.

[53] J. Xu, P. F. J. Lermusiaux, P. J. Haley Jr., W. G. Leslie, and O. G. Logutov. Spatial and Temporal Variations in Acoustic propagation during the PLUSNet-07 Exercise in Dabob Bay. In *Proceedings of Meetings on Acoustics (POMA)*, volume 4, page 11. Acoustical Society of America 155th Meeting, 2008.

[54] Guoqiao You and Shingyu Leung. Eulerian based interpolation schemes for flow map construction and line integral computation with applications to lagrangian coherent structures extraction. *Journal of Scientific Computing*, 74(1):70–96, 2018.

[55] W Zielke, JA Jankowski, J Sündermann, J Segschneider, et al. Numerical modeling of sediment transport caused by deep-sea mining. In *First ISOPE Ocean Mining Symposium*. International Society of Offshore and Polar Engineers, 1995.